

## Two New Flavonoids from *Retama raetam*

by Wen-Hui Xu<sup>a</sup>), Adnan J. Al-Rehaily<sup>\*a</sup>), Muhammad Yousaf<sup>a</sup>), Mohammad S. Ahmad<sup>a</sup>),  
Shabana I. Khan<sup>b</sup>)<sup>c</sup>), and Ikhlas A. Khan<sup>a</sup>)<sup>b</sup>)<sup>c</sup>)

<sup>a</sup>) Department of Pharmacognosy, College of Pharmacy, King Saud University, P.O. Box 2457, Riyadh 11451, Saudi Arabia (phone: +966-11-4673741; fax: +966-11-4677245; e-mail: ajalreha@ksu.edu.sa)

<sup>b</sup>) National Center for Natural Products Research, School of Pharmacy, University of Mississippi, Mississippi, MS 38677, USA

<sup>c</sup>) Department of Pharmacognosy, School of Pharmacy, University of Mississippi, Mississippi, MS 38677, USA

Two new furanoflavonoids, retamasins A and B (**1** and **2**, resp.), along with five known flavonoids, **3**–**7**, were isolated from the aerial parts of *Retama raetam*. Their structures were determined on the basis of extensive spectroscopic (IR, MS, and 1D- and 2D-NMR) analyses and by comparison with the literature data. This is the first report of the isolation of new furanoflavonoids **1** and **2** from *Retama* genus, while compounds **3**, **5**, and **6** were found for the first time from *R. raetam*. Antioxidant and anti-inflammatory activities of the isolated compounds were also evaluated. Compounds **2**, **3**, and **5**–**7** exhibited potent inhibitions of iNOS activity with  $IC_{50}$  values of 2.9, 5.0, 3.1, 1.2, and 4.8  $\mu\text{g/ml}$ , respectively. All compounds inhibited NF- $\kappa$ B except **1** and **5**. Compound **6** was most active in inhibiting iNOS and NF- $\kappa$ B activity, as well as in decreasing oxidative stress.

**Introduction.** – *Retama* is a genus of the plant family Fabaceae, with four species distributed in Mediterranean area, North Africa, and the Canary Islands [1]. *Retama raetam* is an indigenous plant that is common in North and East Mediterranean region and the Sinai Peninsula [2]. The plant flowers from April to May. The molecular and biochemical mechanisms associated with dormancy and drought tolerance in this desert plant have been elucidated [2]. In folk medicine, it is largely recommended by traditional herb practitioners for the management of diabetes [3] and for the treatment of hypertension [4]. In Saudi folk medicine, fruits are particularly used as remedies for diabetes [3]. Experimental studies indicated that *R. raetam* possesses lipid- and body weight-lowering [5], diuretic [6], antihypertensive [7], antioxidant [8], antibacterial [9], and hypoglycemic activities [3]. The confirmation of this traditional usage was demonstrated in both normal and streptozotocin (STZ) rats [3]. In addition, the underlying mechanism of the hypoglycemic effect of *R. raetam* seems to be the stimulation of glycosuria [6].

Previous investigation on *Retama raetam* led to the isolation of a number of compounds, with characteristic compounds being flavonoids [10] and alkaloids [11]. Flavonoids such as daidzein, vicenin-2, naringenin, apigenin, kaempferol, quercetin, and kaempferol-7-*O*-glucoside were found in the seeds [12], and daidzein 7,4'-dimethyl ether, chrysoeriol 7-*O*-glucoside, and orientin in the leaves [13]. Kassem *et al.* isolated two new flavonoids from the aerial part, namely luteolin 4'-*O*-neohesperidoside and 5,4'-dihydroxy-(3'',4''-dihydro-3'',4''-dihydroxy)-2'',2''-dimethylpyrano-(5'',6'':7,8)-flavone [10].

With the aim of identifying further bioactive natural products, a phytochemical investigation focused on its flavonoid constituents was conducted, leading to the isolation of two new furanoflavonoids **1** and **2**, along with five known flavonoids **3–7** (Fig. 1). We report herein the isolation and structure elucidation of the two new compounds, and evaluation of anti-inflammatory and antioxidant activities of all the isolated compounds.

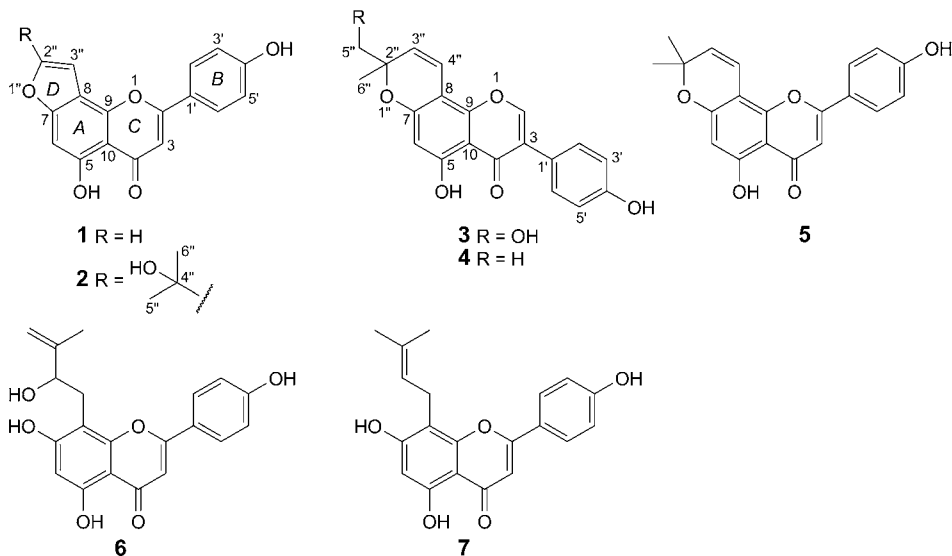


Fig. 1. Structures of compounds **1–7** isolated from *Retama raetam*

**Results and Discussion.** – Compound **1** was obtained as amorphous yellow powder. Its HR-ESI-MS provided the molecular  $\text{C}_{17}\text{H}_{10}\text{O}_5$  (positive-ion mode;  $m/z$  295.0626 ( $[M+H]^+$ ,  $\text{C}_{17}\text{H}_{11}\text{O}_5^+$ ; calc. 295.0603)), indicating 13 degrees of unsaturation in accordance with its  $^{13}\text{C}$ -NMR spectrum displaying 17 resonance signals (Table 1). The BB and DEPT NMR spectra revealed the presence of eight CH groups and nine quaternary C-atoms, including a C=O group ( $\delta(\text{C})$  183.9). The IR spectrum indicated the presence of OH ( $3348\text{ cm}^{-1}$ ) and C=O ( $1655\text{ cm}^{-1}$ ) groups, and a benzene ring ( $1599\text{ cm}^{-1}$ ) *i.e.*, features which were compatible with a flavonoid skeleton [14]. The  $^1\text{H}$ - and  $^{13}\text{C}$ -NMR assignments of compound **1** were based on the COSY, HMQC, and HMBC spectra, as well as on comparison with those previously reported for isopongaglabol [14].

The  $^1\text{H}$ -NMR spectrum (Table 1,  $\text{D}_5$ )pyridine) showed four aromatic H-atom (ring B) signals forming an  $AA'XX'$  system at  $\delta(\text{H})$  8.08 ( $d, J = 8.5$ , H-C(2',6')) and 7.30 ( $d, J = 8.5$ , H-C(3',5')), which suggested the presence of 1,4-disubstituted aromatic ring B. Three *singlets* observed at  $\delta(\text{H})$  13.66, 7.19, and 7.08 were assigned to HO-C(5), H-C(6), and H-C(3), respectively, on the basis of their long-range HMBCs (Fig. 2)  $\delta(\text{H})$  13.66 (HO-C(5))/ $\delta(\text{C})$  159.9 (C(5)), 108.2 (C(10)), and 95.7 (C(6));  $\delta(\text{H})$  7.19 (H-C(6))/ $\delta(\text{C})$  159.9 (C(5)), 159.7 (C(7)), 109.5 (C(8)), and 108.2 (C(10)), and  $\delta(\text{H})$

Table 1.  $^1\text{H}$ - and  $^{13}\text{C}$ -NMR Data (500 and 100 MHz, resp., in  $(\text{D}_5)$ pyridine) of Compounds **1**–**3**<sup>a</sup>.  $\delta$  in ppm,  $J$  in Hz. Atom numbering as indicated in Fig. 1.

Position	<b>1</b>		<b>2</b>		<b>3</b>	
	$\delta(\text{H})$	$\delta(\text{C})$	$\delta(\text{H})$	$\delta(\text{C})$	$\delta(\text{H})$	$\delta(\text{C})$
2		165.0 ( <i>s</i> )		164.8 ( <i>s</i> )	8.09 ( <i>s</i> )	153.8 ( <i>d</i> )
3	7.08 ( <i>s</i> )	104.9 ( <i>d</i> )	7.05 ( <i>s</i> )	105.0 ( <i>d</i> )		123.5 ( <i>s</i> )
4		183.9 ( <i>s</i> )		183.9 ( <i>s</i> )		181.7 ( <i>s</i> )
5		159.9 ( <i>s</i> )		159.2 ( <i>s</i> )		157.9 ( <i>s</i> )
6	7.19 ( <i>s</i> )	95.7 ( <i>d</i> )	7.16 ( <i>s</i> )	95.6 ( <i>d</i> )	6.46 ( <i>s</i> )	95.3 ( <i>d</i> )
7		159.7 ( <i>s</i> )		159.7 ( <i>s</i> )		160.7 ( <i>s</i> )
8		109.5 ( <i>s</i> )		110.4 ( <i>s</i> )		106.2 ( <i>s</i> )
9		149.8 ( <i>s</i> )		149.9 ( <i>s</i> )		157.7 ( <i>s</i> )
10		108.2 ( <i>s</i> )		107.9 ( <i>s</i> )		106.9 ( <i>s</i> )
1'		122.2 ( <i>s</i> )		122.6 ( <i>s</i> )		122.5 ( <i>s</i> )
2',6'	8.08 ( <i>d</i> , $J=8.5$ )	129.3 ( <i>d</i> )	8.07 ( <i>d</i> , $J=8.5$ )	129.4 ( <i>d</i> )	7.72 ( <i>d</i> , $J=8.0$ )	131.4 ( <i>d</i> )
3',5'	7.30 ( <i>d</i> , $J=8.5$ )	117.8 ( <i>d</i> )	7.29 ( <i>d</i> , $J=8.5$ )	117.3 ( <i>d</i> )	7.30 ( <i>d</i> , $J=8.0$ )	116.7 ( <i>d</i> )
4'		163.5 ( <i>s</i> )		163.3 ( <i>s</i> )		159.7 ( <i>s</i> )
2''	7.88 ( <i>d</i> , $J=2.0$ )	145.5 ( <i>d</i> )		165.6 ( <i>s</i> )		82.4 ( <i>s</i> )
3''	7.28 ( <i>d</i> , $J=2.0$ )	105.2 ( <i>d</i> )	7.32 ( <i>s</i> )	98.0 ( <i>d</i> )	5.87 ( <i>d</i> , $J=10.0$ )	126.5 ( <i>d</i> )
4''				68.8 ( <i>s</i> )	7.08 ( <i>d</i> , $J=10.0$ )	117.7 ( <i>d</i> )
5''			1.91 ( <i>s</i> )	29.9 ( <i>q</i> )	4.01 ( <i>d</i> , $J=3.5$ )	69.0 ( <i>t</i> )
6''			1.91 ( <i>s</i> )	29.9 ( <i>q</i> )	1.62 ( <i>s</i> )	24.1 ( <i>q</i> )
5-OH	13.66 ( <i>s</i> )		13.80 ( <i>s</i> )		13.88 ( <i>s</i> )	

<sup>a</sup>) Assignments were based on DEPT and 2D-NMR methods, including DQF-COSY, HMQC, and HMBC.

7.08 (H–C(3))/ $\delta(\text{C})$  183.9 (C(4)), 165.0 (C(2)), 122.2 (C(1')), and 108.2 (C(10)), which indicated a 5-hydroxylated pattern for rings *A* and *C* of flavone skeleton.  $^1\text{H}$ - and  $^{13}\text{C}$ -NMR spectra (Table 1) exhibited characteristic signals ( $\delta(\text{H})/\delta(\text{C})$ ) for a furan ring at  $\delta(\text{H})$  7.88 (*d*,  $J=2.0$ , H–C(2''))/ $\delta(\text{C})$  145.5 (C(2'')) and at  $\delta(\text{H})$  7.28 (*d*,  $J=2.0$ , H–C(3''))/ $\delta(\text{C})$  105.2 (C(3'')) [14]. The three-bond long-range HMBCs (Fig. 2) between H–C(2'') ( $\delta(\text{H})$  7.88) and C(7) ( $\delta(\text{C})$  159.7), and between H–C(2'') ( $\delta(\text{H})$  7.88) and C(8) ( $\delta(\text{C})$  109.5) confirmed that the furan-ring should be along C(7) (O-

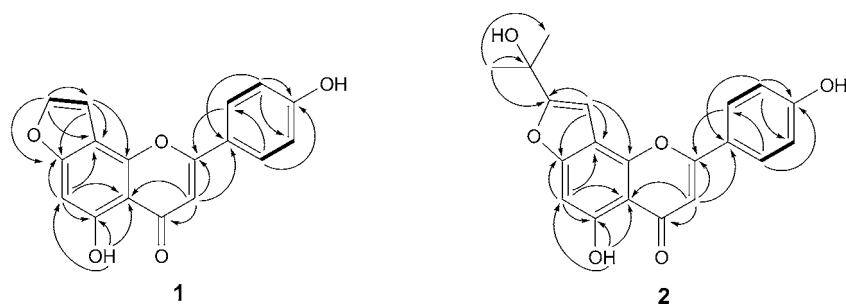


Fig. 2.  $^1\text{H}$ ,  $^1\text{H}$ -COSY (—) and key HMB (H → C) correlations of **1** and **2**

bearing) and C(8) of the aromatic ring. Thus, the structure of **1** was determined as 5-hydroxy-2-(4-hydroxyphenyl)-4*H*-furo[2,3-*h*]-1-benzopyran-4-one, which was named retamasin A.

Compound **2** was isolated as amorphous yellow powder. The HR-ESI-MS showed a *pseudo*-molecular-ion peak for  $[M + H]^+$  at  $m/z$  353.0965 (calc. 353.102) which was 58 mass units (corresponding to an isopropanol moiety) higher than that of compound **1**. In combination with the  $^{13}\text{C}$ -NMR spectrum, the molecular formula of **2** was determined as  $\text{C}_{20}\text{H}_{16}\text{O}_6$ , indicating 13 degrees of unsaturation. The  $^1\text{H}$ - and  $^{13}\text{C}$ -NMR assignments of compound **2** were similar to those previously reported for vogeel except for the furan ring [15]. Comparison of the  $^1\text{H}$ - and  $^{13}\text{C}$ -NMR spectra of **2** with those of **1** indicated that the only difference was the presence of a 1-hydroxy-1-methylethyl moiety at C(2''). The presence of this moiety was evidenced by the  $^1\text{H}$ -NMR signals at  $\delta(\text{H})$  1.91 (s, Me(5'',6'')) and  $^{13}\text{C}$ -NMR signals at  $\delta(\text{C})$  68.8 (C(4'')) and 29.9 (C(5'',6'')). This evidence was further supported by the long-range HMBs  $\delta(\text{H})$  1.91 (H–C(5'')/ $\delta(\text{C})$  165.6 (C(2'')), 68.8 (C(4'')), and 29.9 (C(6'')). Thus, the structure of **2** was established as 5-hydroxy-8-(1-hydroxy-1-methylethyl)-2-(4-hydroxyphenyl)-4*H*-furo[2,3-*h*]-1-benzopyran-4-one and trivially named retamasin B.

In addition to **1** and **2**, five known compounds were also isolated from the  $\text{CHCl}_3$  extract of *R. raetam*. By comparison of their physical, and EI-MS and NMR data with those reported in literature, the known compounds were identified as hydroxyderrone (**3**) [16], derrone (**4**) [17], atalantoflavone (**5**) [18], ephedroidin (**6**) [19], and licoflavone C (**7**) (Fig. 1) [20]. To the best of our knowledge, this is the first report of the isolation of furanoflavonoids from *Retama* genus, while compounds **3**, **5**, and **6** were isolated from *R. raetam* for the first time [21][22]. In addition, compound **3** was previously isolated from *Ficus auriculata* [16], and its structure was determined by limited spectroscopic data; however, this is the first report containing the complete NMR data of **3** in ( $\text{D}_5$ )pyridine.

Due to the history of use of this plant as remedy for diabetes and previous reports of its antidiabetic action [5], we explored the anti-inflammatory properties of the constituents isolated in this study. Inflammation is the response of living cells and tissues to injury, and it usually comprises a complex combination of enzyme activation, mediator release, extravasations of fluid, cell migration, and tissue breakdown and repair [23]. Inflammation is an important component of metabolic syndrome which includes conditions such as several types of cancer, diabetes, obesity, and metabolic disorders. The activation of NF- $\kappa$ B in response to pro-inflammatory signals is associated with many diseases caused by unregulated inflammation. Since NF- $\kappa$ B is highly activated at the sites of inflammation in diverse diseases, the compounds that can suppress NF- $\kappa$ B activation have potential as anti-inflammatory agents [24]. Excessive generation of nitric oxide (NO) and reactive oxygen species (ROS) also contributes significantly to the progress of inflammation and development of metabolic syndrome, characterized by obesity, diabetes, and cardiovascular diseases. Inhibition of inducible nitric oxide synthase (iNOS) can reduce the intracellular NO production. NF- $\kappa$ B, iNOS, and ROS have been considered as important targets for inflammation [25]. We evaluated anti-inflammatory activities of isolated compounds in terms of their effects on oxidative stress, and iNOS, and NF- $\kappa$ B activities. A decrease in cellular oxidative stress was observed in response to several of these flavonoids as shown in Table 2.

Table 2. Antioxidant and Anti-Inflammatory Activities of Flavonoids 1–7 from *Retama raetam*

Compound	Decrease in oxidative stress at 500 µg/ml [%]	$IC_{50}$ [µg/ml]	
		Inhibition of iNOS	Inhibition of NF-κB
<b>1</b>	NA <sup>a)</sup>	7.4	NA
<b>2</b>	46	2.9	16
<b>3</b>	42	5	12.5
<b>4</b>	50	18	13.5
<b>5</b>	22	3.1	NA
<b>6</b>	60	1.2	8
<b>7</b>	NA	4.8	11.5
Quercetin	50	NT	NT
Parthenolide	NT <sup>b)</sup>	0.5	1.5

<sup>a)</sup> NA, Not active. <sup>b)</sup> NT, Not tested.

Compounds **2–4** and **6** showed a decrease of 42–60% in the oxidative stress at 500 µg/ml concentration in a cellular antioxidant assay using ABAP-induced HepG2 cells. The results indicated their antioxidant activity is in accordance with the previous literature [26]. Quercetin, used as a positive control, showed a 50% decrease in oxidative stress at 3.02 µg/ml concentration.

All the flavonoids showed inhibition of iNOS activity. Compounds **2**, **3**, and **5–7** were more active than **1** and **4**. They inhibited iNOS activity with  $IC_{50}$  values in the range of 1.2–5 µg/ml in lipopolysaccharide (LPS)-induced macrophages.

Compound **1** and **4** inhibited iNOS activity with  $IC_{50}$  values of 7.4 and 18 µg/ml, respectively. The  $IC_{50}$  value for parthenolide, as a positive control, was 0.5 µg/ml.

The inhibition of NF-κB was determined in phorbol 12-myristate 13-acetate (PMA)-induced SW1353 cells by a reporter gene assay.

All the flavonoids inhibited transcriptional activity of NF-κB except **1** and **5** as shown in Table 2. Compound **6** was the most effective in inhibiting the NF-κB activity with an  $IC_{50}$  value of 8 µg/ml, while compounds **3**, **4**, and **7** displayed  $IC_{50}$  values of 12.5, 13.5, and 11.5 µg/ml, respectively. The  $IC_{50}$  value of the positive control, parthenolide, was 1.5 µg/ml in the same assay.

These results indicate that the flavonoids present in *R. raetam* possess anti-inflammatory activities in terms of multiple targets, contributing to the beneficial effects of this plant. The plant seems to have anti-inflammatory potential in addition to its traditional use against diabetes and metabolic disorders.

### Experimental Part

*General.* TLC: Silica-gel sheets (SiO<sub>2</sub>; *Alugram Sil G/UV254*; *Macherey–Nagel*; Germany) and reversed-phase (RP) plates (*RP-18 F254S*; *Merck*; Germany); visualization with 10% H<sub>2</sub>SO<sub>4</sub>, followed by heating. Column chromatography (CC): normal-phase SiO<sub>2</sub> (*Merck*; 230–400 µm) and RP SiO<sub>2</sub> (*LiChroprep RP-18*; *Merck*; 40–63 µm). HPLC: *Shimadzu* system (Kyoto, Japan), consisting of two *LC-6AD Semi-Prep. Solvent Delivery* pumps coupled with *Rheodyne* manual injector; communications bus module *CBM-20A*; a multi-wavelength photo-diode array detector (*SPD-M20A*); *FRC-10A* fraction collector, all connected to a computer system with *Intel Core DUO* with *Microsoft XP* and *Shimadzu's*

LC solution software. It was fitted with a *Shim-pack PREP-ODS(H) Kit* 250 mm  $\times$  4.6 mm i.d. with 5- $\mu$ m particles (A), and 250 mm  $\times$  20 mm i.d., 5- $\mu$ m particles (B). Anal. HPLC: column A under gradient conditions with a mobile phase consisting of MeCN/H<sub>2</sub>O 40:60 programmed linearly to 100% MeCN over 25 min at the flow rate of 1.0 ml/min. The UV detection wavelength was 254 nm. The HPLC analyses were performed using column B, and prep. HPLC conditions were the same as those of anal. HPLC except the flow rate (20 ml/min). UV Spectra: *HP 8453* diode array spectrophotometer;  $\lambda_{\max}$  ( $\epsilon$ ) in nm. IR Spectra: *PerkinElmer FT-IR 600* series spectrometer; KBr pellets;  $\tilde{\nu}$  in cm<sup>-1</sup>. 1D- and 2D-NMR (DQF-COSY, HMQC, HMBC) spectra: *Bruker Avance DRX 500* FT spectrometer operating at 500 (<sup>1</sup>H) and 125 (<sup>13</sup>C) MHz at r.t.;  $\delta$  in ppm rel. to Me<sub>4</sub>Si as internal standard,  $J$  in Hz. HR-EIS-MS: *Agilent Series 1100 SL* mass spectrometer, in  $m/z$ .

**Plant Material.** The aerial parts of *Retama raetam* were collected in April, 2010, from Al-looz Mountain, Tabook, Saudi Arabia, and identified by Dr. M. Yusuf, taxonomist, College of Pharmacy, King Saud University (KSU), Riyadh, Saudi Arabia. A voucher specimen (No.15567) was deposited with the herbarium of the College of Pharmacy, KSU.

**Extraction and Isolation.** The air-dried aerial parts (1.5 kg) of *Retama raetam* were percolated at r.t. with CHCl<sub>3</sub> (3  $\times$  31, 24 h each) to yield a dark brown residue (26.0 g). This extract was partitioned between hexane and MeCN to afford a hexane fraction (8.0 g) and a MeCN fraction (11.0 g). The MeCN fraction (11.0 g) was subjected to CC (SiO<sub>2</sub> 5.5  $\times$  50 cm); linear gradient elution with MeOH and acetone to give 17 pooled fractions, *Fr. A–Q*. *Fr. K* (144 mg) was purified by RP CC (SiO<sub>2</sub>; MeOH/H<sub>2</sub>O 80:20–100:0) to furnish **1** (12.0 mg) and **5** (8.0 mg). *Fr. O* (514 mg) was further purified by RP CC (C<sub>18</sub>; MeOH/H<sub>2</sub>O 65:35–100:0) to afford **2** (24.0 mg) and **6** (30.0 mg). *Fr. M* (490 mg) was purified by RP CC (SiO<sub>2</sub>; MeOH/H<sub>2</sub>O 70:30–100:0) to give **3** (21.0 mg) and **7** (14.0 mg). *Fr. H* (247 mg) was further separated by RP CC (C<sub>18</sub>; MeOH/H<sub>2</sub>O 70:30–100:0) to yield **4** (20.0 mg).

**Retamasin A** (=5-Hydroxy-2-(4-hydroxyphenyl)-4H-furo[2,3-h]-1-benzopyran-4-one; **1**). Amorphous yellow powder. UV (MeOH): 315 (4819), 265 (4378). IR (KBr): 3348, 1655, 1603, 1599, 1514, 1448, 1358, 1263, 1171, 1054, 932, 812. <sup>1</sup>H- and <sup>13</sup>C-NMR: see *Table 1*. HR-ESI-MS: 295.0626 ( $[M + H]^+$ , C<sub>17</sub>H<sub>11</sub>O<sub>5</sub><sup>+</sup>; calc. 295.0603).

**Retamasin B** (=5-Hydroxy-8-(1-hydroxy-1-methylethyl)-2-(4-hydroxyphenyl)-4H-furo[2,3-h]-1-benzopyran-4-one; **2**). Amorphous yellow powder. UV (MeOH): 315 (3926), 265 (3751). IR (KBr): 3347, 1653, 1541, 1457, 1054. <sup>1</sup>H- and <sup>13</sup>C-NMR: see *Table 1*. HR-ESI-MS: 353.0965 ( $[M + H]^+$ , C<sub>20</sub>H<sub>17</sub>O<sub>6</sub><sup>+</sup>; calc. 353.102).

**Reporter-Gene Assay for the Inhibition of NF- $\kappa$ B Activity.** Human chondrosarcoma (SW1353) cells were cultured in *Dulbecco's modified Eagle's medium* (DMEM)/F12 medium supplemented with 10% fetal bovine serum (FBS), 100 U/ml penicillin G sodium, and 100  $\mu$ g/ml streptomycin at 37° in an atmosphere of 5% CO<sub>2</sub> and 95% humidity. The assay was performed as described in [27]. In brief, cells transfected with NF- $\kappa$ B luciferase plasmid construct were plated in 96-well plates at a density of 1.25  $\times$  10<sup>5</sup> cells/well. After 24 h, cells were treated with the test compounds, and, after incubating for 30 min, phorbol 12-myristate 13-acetate (PMA; *Sigma–Aldrich*; 70 ng/ml) was added and further incubated for 6–8 h. Luciferase activity was measured using a *Luciferase Assay Kit* (*Promega*, Madison, WI, USA). Light output was detected on a *SpectraMax* plate reader. Percent decrease in luciferase activity was calculated relative to the vehicle control. Parthenolide (*Sigma–Aldrich*) was used as a positive control.

**Assay for Inhibition of iNOS Activity.** The assay was performed with mouse macrophages (RAW264.7) cultured in phenol red-free RPMI medium with 10% bovine calf serum, 100 U/ml penicillin G sodium, and 100  $\mu$ g/ml streptomycin. Cells were seeded in 96-well plates (100,000 cells/well) and incubated for 24 h for a confluency of 75% or more. The cells were treated with the test compounds, and, after 30 min, LPS (*Sigma–Aldrich*; 5  $\mu$ g/ml) was added and further incubated for 24 h. The activity of iNOS was determined in terms of the concentration of NO by measuring the level of nitrite in the cell culture supernatant using *Griess* reagent (*Sigma–Aldrich*). Percent inhibition of nitrite production by the test compound was calculated in comparison to the vehicle control. The IC<sub>50</sub> values were obtained from dose–response curves. Parthenolide was used as the positive control [28].

**Assay for Inhibition of Cellular Oxidative Stress.** The cellular antioxidant activity was measured in HepG2 cells as described in [29]. The method allows measurement of the ability of test compounds to prevent intracellular generation of peroxy radicals in response to 2,2'-azobis(2-amidinopropane)

dihydrochloride (ABAP, *Sigma–Aldrich*), a generator of peroxy radicals. The assay is more relevant biologically than as a chemical assay, because it represents the complexity of a biological system and accounts for cellular uptake, bioavailability, and metabolism of the antioxidant agent being tested. For the assay, HepG2 cells were seeded in the wells of a 96-well plate at a density of 60,000 cells/well and incubated for 24 h. The medium was removed, and cells were washed with PBS (phosphate-buffered saline) before treating with the test compounds diluted in serum-free medium containing 25  $\mu\text{M}$  2',7'-dichlorofluorescein diacetate (DCFH-DA; *Invitrogen*, Carlsbad, CA, USA) for 1 h. After removing the medium, the cells were treated with 600  $\mu\text{M}$  ABAP, and the plate was immediately placed on a *SpectraMax* plate reader for kinetic measurement every 5 min for 1 h (37°; emission at 538 nm and excitation at 485 nm). Quercetin (*Sigma–Aldrich*) was included as the positive control. The area under the curve (AUC) of fluorescence vs. time was used to calculate cellular antioxidant activity (CAA) units according to the following equation:

$$\text{CAA unit} = 100 - [(\text{AUC}(\text{sample})/\text{AUC}(\text{control})) \times 100] \quad (1)$$

The  $IC_{50}$  values of the test samples were calculated from dose–response curves of CAA units vs. test concentration. Quercetin at 10  $\mu\text{M}$  caused 50% inhibition of cellular generation of peroxy radicals in HepG2 cells.

#### REFERENCES

- [1] C. Martín-Cordero, M. López-Lázaro, J. L. Espartero, M. J. Ayuso, *J. Nat. Prod.* **2000**, *63*, 248.
- [2] R. Mittler, E. Merquiol, E. Hallak-Herr, S. Rachmilevitch, A. Kaplan, M. Cohen, *Plant J.* **2001**, *25*, 407.
- [3] M. Maghrani, A. Lemhadri, H. Jouad, J. B. Michel, M. Eddouks, *J. Ethnopharmacol.* **2003**, *87*, 21.
- [4] O. Ishurd, A. Kermagi, F. Zgheel, M. Flefla, M. Elmabruk, Y. L. Wu, J. F. Kennedy, Y. J. Pan, *Carbohydr. Polym.* **2004**, *58*, 41.
- [5] M. Maghrani, A. Lemhadri, N. A. Zeggwagh, A. El Amraoui, M. Haloui, H. Jouad, M. Eddouks, *J. Ethnopharmacol.* **2004**, *90*, 323.
- [6] M. Maghrani, N. A. Zeggwagh, M. Haloui, M. Eddouks, *J. Ethnopharmacol.* **2005**, *99*, 31.
- [7] M. Eddouks, M. Maghrani, L. Louedec, M. Haloui, J. B. Michel, *J. Herb. Pharmacother.* **2007**, *7*, 65.
- [8] F. Conforti, G. Statti, R. Tundis, M. R. Loizzo, M. Bonesi, F. Menichini, P. J. Houghton, *Phytother. Res.* **2004**, *18*, 585.
- [9] E. Hayet, A. Samia, G. Patrick, M. M. Ali, M. Maha, G. Laurent, Z. Mighri, L. Mahjoub, *Pak. J. Biol. Sci.* **2007**, *10*, 1759.
- [10] M. Kassem, S. A. Mosharrafa, N. A. M. Saleh, M. Abdel-Wahab, *Fitoterapia* **2000**, *71*, 649.
- [11] A. El-Shazly, A. M. Ateya, L. Witte, M. Wink, *Z. Naturforsch. C* **1996**, *51*, 301.
- [12] A. O. B. Halim, H. Abdel Fattah, A. F. Halim, I. Murakoshi, *Acta Pharm. Hung.* **1997**, *67*, 241.
- [13] M. A. M. Nawwar, A. E. A. El Sherbeiny, M. A. El Ansari, *Cell. Mol. Life Sci.* **1975**, *31*, 1118.
- [14] S. K. Talapatra, A. K. Mallik, B. Talapatra, *Phytochemistry* **1982**, *21*, 761.
- [15] M. I. Ali, Z. Ahmed, F. K. A. Waffo, M. S. Ali, *Nat. Prod. Commun.* **2010**, *5*, 889.
- [16] C. R. Han, J. C. Zhang, X. P. Song, C. J. Zheng, T. M. Shao, C. Y. Dai, China Pat. CN 103450209 A, 2013.
- [17] S. S. Chibber, R. P. Sharma, *Phytochemistry* **1980**, *19*, 1857.
- [18] A. Banerji, D. L. Luthria, B. R. Prabhu, *Phytochemistry* **1988**, *27*, 3637.
- [19] L. Pistelli, A. Bertoli, I. Giachi, A. Manunta, *J. Nat. Prod.* **1998**, *61*, 1404.
- [20] A. R. Han, Y. J. Kang, T. Windono, S. K. Lee, E. K. Seo, *J. Nat. Prod.* **2006**, *69*, 719.
- [21] R. Maurya, P. P. Yadav, *Nat. Prod. Rep.* **2005**, *22*, 400.
- [22] N. C. Veitch, R. J. Grayer, *Nat. Prod. Rep.* **2008**, *25*, 555–611.
- [23] J. B. Perianayagam, S. K. Sharma, K. K. Pillai, *J. Ethnopharmacol.* **2006**, *104*, 410.
- [24] P. P. Tak, G. S. Firestein, *J. Clin. Invest.* **2001**, *107*, 7.
- [25] J. K. Ko, K. K. Auyeung, *Curr. Pharm. Des.* **2013**, *19*, 48.
- [26] D. A. Okoth, H. Y. Chenia, N. A. Koorbanally, *Phytochem. Lett.* **2013**, *6*, 476.

- [27] G. Ma, S. Khan, G. Benavides, W. Schuehly, N. Fischer, I. Khan, D. Pasco, *Cancer Chemother. Pharmacol.* **2007**, *60*, 35.
- [28] M. A. Zaki, P. Balachandran, S. Khan, M. Wang, R. Mohammed, M. H. Hetta, D. S. Pasco, I. Muhammad, *J. Nat. Prod.* **2013**, *76*, 679.
- [29] K. L. Wolfe, H. L. Rui, *J. Agric. Food Chem.* **2007**, *55*, 8896.

*Received October 2, 2014*